Published in final edited form as:
Regen Med. 2012 May ; 7(3): 323–334. doi:10.2217/rme.12.13.

Subcellular preconditioning of stem cells: mito-Cx43 gene targeting is cytoprotective via shift of mitochondrial Bak and Bcl-xL balance

Gang Lu, **Shujia Jiang**, **Muhammad Ashraf**, and **Khawaja Husnain Haider***
Department of Pathology & Laboratory Medicine, University of Cincinnati, 231 Albert Sabin Way, Cincinnati, OH 45267, USA

Abstract

Aim—To achieve mitochondria-specific expression of connexin-43 (*Cx43*) transgene for mitochondrial preconditioning in stem cells to improve their survival post-transplantation during heart cell therapy.

Methods & results—Cx43- or GFP-encoding adenoviral vectors with a mitochondrial targeting sequence were constructed for transduction of bone marrow Sca-1$^+$ cells (>90% transduction efficiency). Double-fluorescence immunostaining for cytochrome-c and Cx43 supported by western blotting confirmed mitochondria-specific Cx43 expression in adenoviral-mito-Cx43-transduced cells (^{Cx43}Sca-1$^+$). ^{Cx43}Sca-1$^+$ showed improved survival under lethal oxygen–glucose deprivation culture conditions. ^{Cx43}Sca-1$^+$ showed an increased mitochondrial Bcl-xL:Bak ratio and reduced cytochrome-c release into cytosol with concomitantly abolished caspase-3 activity. An *in vivo* study was performed such that 2×10^6 male ^{Cx43}Sca-1$^+$ or ^{GFP}Sca-1$^+$ cells were injected into a female rat model of acute myocardial infarction. DMEM-injected rats served as controls. On day 7 post-transplantation, 4.3-fold higher survival of ^{Cx43}Sca-1$^+$ cells ($p < 0.05$ vs control) and reduced terminal deoxynucleotidyl transferase dUTP nick end labeling positivity in the left ventricle (LV) were observed. In comparison, LV ejection fraction (40.2 ± 0.9%), LV fractional shortening (20.0 ± 1.6%) and LV end diastolic dimension (6.5 ± 0.3 mm) were observed in ^{GFP}Sca-1$^+$, and treatment with ^{Cx43}Sca-1$^+$ cells improved these parameters (47.6 ± 2.5%, $p < 0.05$; 27.7 ± 1.2%, $p < 0.05$; and 5.6 ± 0.1 mm, $p < 0.05$, respectively), along with concomitant reductions in infarction size (33.7 ± 2.9% vs 39.8 ± 1.4%; $p < 0.05$).

Conclusion—Mitochondria-targeted Cx43 expression is a novel approach to improve stem cell survival in the infarcted heart.

*Author for correspondence: Tel.: +1 513 558 0145, Fax: +1 513 558 0807, haiderkh@ucmail.uc.edu.

Ethical conduct of research
The authors state that they have obtained appropriate institutional review board approval or have followed the principles outlined in the Declaration of Helsinki for all human or animal experimental investigations. In addition, for investigations involving human subjects, informed consent has been obtained from the participants involved.

Financial & competing interests disclosure
This work was supported by NIH grants R37HL074272, HL-080686 and HL-087246 (to M Ashraf) and HL-087288, HL-089535 and HL106190-01 (to KH Haider). The authors have no other relevant affiliations or financial involvement with any organization or entity with a financial interest in or financial conflict with the subject matter or materials discussed in the manuscript apart from those disclosed.
No writing assistance was utilized in the production of this manuscript.

Keywords

connexin-43; infarction; mitochondria; stem cell; survival

Connexin-43 (Cx43) is an integral constituent protein of the gap junctions with exclusive distribution in the sarcolema and ensures intercellular communication, including molecular transfer and conduction of electrical signals [1]. The presence of Cx43 in the mitochondria (mito-Cx43) is being recognized as having a cytoprotective role during preconditioning and in response to ischemia reperfusion injury [2–6]. Recent studies have reported stress-altered subcellular distribution of Cx43, which implies a prosurvival function of Cx43 independent of its gap junction activity [1,7–10]. There is mounting evidence that Cx43 is translocated into the mitochondria in response to oxidative stress and opening of mitochondria K^+ ATP channels as part of pro-survival activity in the cells [2,4,11–13]. Despite these encouraging data, the molecular mechanism involved therein has not been fully elucidated. We have reported that preconditioning of stem cells with IGF-1 improved their survival under ischemic stress and post-transplantation in the infarcted animal hearts with concomitant translocation of Cx43 into the mitochondria [14]. PKCα and Erk1/2 activation in stem cells cultured under oxygen–glucose deprivation (OGD) becomes accentuated in response to short-term IGF-1 treatment during preconditioning [15]. Abrogation of Erk1/2 abolished mitochondrial translocation of Cx43 with simultaneous loss of the cytoprotective effects of IGF-1. Given the significance of mito-Cx43 in cytoprotection, we hypothesized that mitochondrial preconditioning in stem cells by specific targeting of the *Cx43* transgene would be a novel subcellular preconditioning approach to improve their survival [16].

Given their crucial role in the maintenance of cellular homeostasis, the mitochondria have been extensively studied for their participation in cell survival signaling [17]. More recent focus in this regard has fallen on the involvement of mito-Cx43, either already present in the inner mitochondrial membrane [18] or translocated in response to preconditioning [14], in cell survival signaling. However, the exact mechanism by which mito-Cx43 promotes cell survival remains an area of intense investigation. Our strategy of mitochondria-specific targeting of the *Cx43* trans-gene provides a proof-of-concept and highlights the antiapoptotic significance of mitochondrial Cx43. Although our strategy of mitochondrial targeting of a Cx43 plasmid using a nonviral vector simulated the prosurvival effects of preconditioning with IGF-1, low transfection efficiency was a limiting factor that hindered its optimal beneficial effects. The study also did not provide *in vivo* evidence regarding the prosurvival effects of mito-Cx43. The present study was therefore aimed to address both these limitations by developing a high-efficiency adenoviral (Ad) vector encoding for the *Cx43* transgene with a mitochondria-specific localization signal, as well as determining the prosurvival effects of mitochondria-specific Cx43 overexpression in stem cells. We have also elucidated a relationship between mito-Cx43 and Bcl-2 family members. Our results showed that mitochondrial targeting of Cx43 prevented cytochrome-c release and altered the balance of anti- and pro-apoptotic Bcl-2 family members between mitochondrial and cytoplasmic compartments of stem cells, a molecular event that was integral to cytochrome-c release from the mitochondria during the onset of apoptosis. The strategy of sub-cellular mitochondrial preconditioning by targeting of *Cx43* transgene would therefore be a novel therapeutic approach to support stem cell survival postengraftment in the ischemic heart.

Materials & methods

Isolation & culture of bone marrow Sca-1$^+$ cells

The study conforms to the Guide for the Care and Use of Laboratory Animals published by the US NIH (publication no. 85-23, revised 1985) and protocols approved by the Institutional Animal Care and Use Committee, University of Cincinnati (OH, USA).

Bone marrow Sca-1$^+$ cells were isolated from 6–8-week-old male C57BL/6 mice [14] and purified using a Sca-1$^+$ cell isolation kit (Stem Cell Technologies, Inc., BC, Canada) per manufacturer's instructions. The purified cells were propagated as previously described [14].

Construction of viral vectors for mitochondria-specific transgene delivery

Ad vectors were constructed with AdEasy™ XL Adenoviral Vector System (Stratagene, CA, USA) [19]. Ad encoding for mitochondria-targeted Cx43 and GFP were also constructed with the AdEasy XL Adenoviral Vector System [16]. Briefly, pShuttle vectors were linearized with Pme-I and were gel purified. The purified products were transformed into BJ5183-AD-1 cells, which carried viral backbone vector by electroporation. Transformants were plated onto lysogeny broth (LB) agar containing kanamycin and at least ten small colonies were picked from the plate and inoculated into 3 ml of LB kanamycin broth and cultured in a shaker incubator at 37°C. Miniprep DNA from overnight culture was harvested by the conventional alkaline lysis method and digested with Pac-I. Recombinant viral plasmid DNA was confirmed with agarose gel electrophoresis to yield a large fragment of 30 kb and a small fragment of either 3.0 or 4.5 kb. Minipreped recombinant plasmids were retransformed into XL-10 Gold® Ultracompetent cells (Strategene) and plated on agar plates containing kanamycin. Single colonies were inoculated into 100 ml LB kanamycin for overnight culture. Plasmid midiprep was performed with the Qiagen (CA, USA) midiprep kit. Midiprep recombinant viral vector (5 μg) was digested with Pac-I and transfected into AD-293 cells plated on 25-cm^2 tissue culture flasks. The cells were observed for GFP expression. The primary viral stock was used for amplification of new AD-293 cells. Primary viral stock was subjected to three more rounds of amplification to achieve a high titer viral stock and viral vector was purified with Adeno-X™ Maxi Purification Kit (Clontech Labs, Inc., CA, USA).

OGD & cell survival

Sca-1$^+$ cells were grown in DMEM containing 20% fetal bovine serum until they reached approximately 70–80% confluence. Culture medium was removed and cells were rinsed three times with glucose and sodium pyruvate-free DMEM (Invitrogen, CA, USA) and cells were cultured at 37°C in an airtight anoxia chamber (In Vivo$_2$-500; Ruskinn, UK) saturated with 95% N_2/5% CO_2 for up to 8 h. Intracellular lactate dehydrogenase release was measured using Homogeneous Membrane Integrity Assay (Promega, WI, USA) as an indicator of cell membrane integrity and cell viability. Terminal deoxynucleotidyl transferase dUTP nick end labeling (TUNEL) assay was performed with an *in situ* cell death detection kit (TMR Red; Roche Applied Science, Germany).

Caspase-3 activity assay

Sca-1$^+$ cells were exposed to OGD and cell lysates were collected. Caspase-3 activity was measured with a caspase-3 immunoassay kit per instructions of the manufacturer (EMD Bioscience, CA, USA).

Mitochondria fractionation

Mitochondrial fractionation was performed with ProteoExtract® Cytosol/Mitochondria Fractionation Kit (EMD Bioscience) per manufacturer's instruction and as described previously [16].

Western blot analysis

Protein concentration of the cell lysate samples from cytosolic and mitochondrial fractions was determined by Lowry's method. Western blotting was performed as previously described [15]. Antibodies used included anti-FLAG (1:5000; Sigma-Aldrich, MO, USA), anti-Cx43, anti-VDAC (1:5000; Abcam, CA, USA), anti-Cox IV (1:10,000; Abcam), anti-Bcl-xL, anti-Bak, anti-Bax (1:4000; Cell Signaling, MA, USA), anti-cytochorme-c (1:2000; BD Bioscience, MD, USA) and anti-actin (1:4000; Santa Cruz Biotechnology, CA, USA) [15].

Fluorescence immunostaining

The samples were fixed with 4% paraformal-dehyde at room temperature for 5 min followed by 5 min permeabilization with 0.2% Triton™ X-100 (Sigma, MO, USA). Blocking was performed at room temperature for 30 min with 10% animal serum from the same animal species as secondary antibodies. Primary and secondary antibodies were diluted in blocking buffer and were incubated at room temperature for 45 and 30 min, respectively. Every time after incubation with antibody, the samples were washed three times with phosphate-buffered saline. The nuclei were stained with DAPI and after mounting with Fluoromount G™ (Southern Biotech, AL, USA), images were taken with a fluorescence microscope (BX-41; Olympus, Japan) or using a confocal microscope (Leica, Germany).

Acute myocardial infarction & cell transplantation

The experimental animal model of acute coronary artery ligation was developed in young (6–8 weeks of age) female Fischer rats [14]. The animals were anesthetized by intraperitoneal injection of ketamine/xylazine (87 mg/kg and 13 mg/kg, respectively). After endotracheal intubation and ventilation using a Harvard Rodent Ventilator (Model 683), the heart was exposed via minimal left-sided thoracotomy. The left anterior descending coronary artery was occluded using a Prolene™ 6-0 (Ethicon, TX, USA) suture at 1–2 mm lower than the tip of the left atrium. Myocardial infarction was confirmed by immediate pallor of the left ventricle (LV) free wall. The animals were grouped to receive intramyocardial injections of 70 μl of DMEM without cells (group 1) or 2×10^6 male Sca-1^+ cells infected with Ad-mito-GFP-FLAG (^{GFP}Sca-1^+ cell-treated group 2; control) or Sca-1^+ cells infected with Ad-mito-Cx43-FLAG (^{Cx43}Sca-1^+ cell-treated group 3). The chest of the animal was sutured and the animal was allowed to recover in an oxygen-perfused chamber. The animals were treated with Buprenex® (Reckitt Benckiser Pharmaceutical Inc., NJ, USA; 0.1 mg/kg twice daily) for pain management during the first 24 h after surgery. The animals were assessed for heart function at 4 weeks after their respective treatment before euthanasia, and the heart tissue was collected for histological and immunohistological studies. Six animals each in groups 2 and 3 and four animals in the DMEM-treated group 1 were also euthanized on day 7 after their respective treatment and were used for molecular as well as short-term histological studies.

Cell survival studies *in vivo* by real-time PCR

The survival of the sex-mismatched male donor cells in the female recipient hearts was performed by *sry* gene analysis, as described previously [14]. Briefly, genomic DNA from the heart tissue samples collected on day 7 after treatment was extracted using a Genomic DNA extraction Kit (Qiagen). The amount of DNA was quantified with a

spectrophotometer. The primers used to amplify the mouse *sry* gene were purchased from Qiagen (Cat#: QT01038555) [14]. Real-time PCR was performed with SYBR® Green Master Mix (Qiagen), 200 ng genomic DNA and *sry* primers using Bio-Rad iQ-5 iCycler® (Bio-Rad Laboratories, CA, USA), and the program was run as: denaturation at 95°C for 15 min, 45 cycles of 95°C for 15 s, 55°C for 30 s and 72°C for 30 s. Upon completion of PCR, a melting curve was run from 55 to 95°C, with an increment of 1°C and a dwelling time of 15 s to verify the purity of the amplification product [14].

Transthoracic echocardiography & measurement of infarction size

Transthoracic echocardiography was performed to evaluate the improvements of heart function of rats after cell transplantation [14]. Rats were anesthetized with ketamine/xylazine and placed in the supine position. Hearts were imaged in 2D and M-mode, and recordings were obtained from parasternal long-axis view at papillary muscle level using Compact Linear Array probe CL10-5 on an HDI-5000/SONOS-CT (Phillips, Washington, DC, USA). Anterior and posterior end diastolic and end systolic wall thickness, LV end systolic diameter (LVESD) and LV end diastolic diameter (LVEDD) were measured from at least three consecutive cardiac cycles. Indices of LV systolic functions, including LV fractional shortening (LVFS) and LV ejection fraction (LVEF), were calculated using the following equations:

$$\mathrm{LVFS}=(\mathrm{LVEDD}-\mathrm{LVSED})/\mathrm{LVEDD}\times 100$$

$$\mathrm{LVEF}=([\mathrm{LVEDD}^3-\mathrm{LVESD}^3]/\mathrm{LVEDD}^3)\times 100$$

Statistical analysis

All data were expressed as means ± standard errors of the mean. The comparison among different treatment groups were made using the Student's t-test or analysis of variance with a mixed-effect model to account for random effects from different repetition and unequal variance. A value of $p \leq 0.05$ was considered as statistically significant.

Results

Characterization of ^{Cx43}Sca-1$^+$ cells

Ad vectors carrying the mitochondria-targeted GFP and Cx43 were successfully constructed with corresponding pShuttle vectors (Figure 1A). The second open reading frame encoded humanized GFP, which served as an indicator of successful transgene delivery and expression. Transduction efficiency with either Ad-mito-GFP-FLAG or Ad-mito-Cx43-FLAG was nearly 100% (Figure 1B). For quantitative determination of transgene expression, Sca-1$^+$ cells were infected with a series of doses of Ad-mito-GFP-FLAG or Ad-mito-Cx43-FLAG, and FLAG fusion protein expression was detected by western blots, which showed a direct relationship between FLAG expression and vector dose (Figure 1C). Moreover, Sca-1$^+$ cells infected with 5, 10 and 20 μl of Ad-mito-Cx43-FLAG expressed similar amount of FLAG protein as Sca-1$^+$ cells infected with 20, 50 and 100 μl of 1:50 diluted Ad-mito-GFP-FLAG, respectively (Figure 1C). These results were confirmed by immunostaining (Figure 1D). An appreciable increase in FLAG expression (red) was observed with increasing amounts of viral vector. These results showed that when GFP was detectable in Ad-mito-GFP-FLAG-transduced cells, FLAG had already started to show off-target expression. Therefore, our dose–response studies helped us to optimize the Ad-mito-Cx43-FLAG and Ad-mito-GFP-FLAG vector dose where two vectors produced equivalent

responses in terms of FLAG expression and avoided off-target transgene expression. Confocal imaging after double-fluorescence immunostaining of ^{Cx43}Sca-1^{+} for FLAG (red) revealed punctuate FLAG distribution, which colocalized with cytochrome-c expression (green; Figure 1E). Western blots of mitochondrial protein fractions confirmed that FLAG and Cx43 were localized in the mitochondria (Figure 1F). Cox IV was used as a control.

Mitochondria-specific Cx43 expression & cytoprotection

^{Cx43}Sca-1^{+} cells and ^{GFP}Sca-1^{+} cells transduced with different concentrations of respective viral vectors were subjected to 6 and 8 h OGD. Lactate dehydrogenase release was significantly reduced at both time-points in ^{Cx43}Sca-1^{+} cells (Figure 2A & 2B). The three different doses of Ad vectors used for transduction showed comparable cytoprotective effects. Phase-contrast images at 4 and 8 h after OGD showed that ^{Cx43}Sca-1^{+} cells had better-preserved morphology (Figure 2C), reduced TUNEL positivity (Figure 2D) and low caspase-3 activity ($p < 0.01$ vs ^{GFP}Sca-1^{+}; Figure 2E).

We next sought to elucidate the signaling mechanism by which mitochondrial Cx43 conferred cytoprotection. Bcl-2 family members Bax and Bak are essential constituents of mitochondria outer membrane pores (MOMPs), which facilitates cytochrome-c release [20]. To study the baseline response to OGD, native Sca-1^{+} cells were subjected to 4 and 8 h OGD using Sca-1^{+} cells without OGD treatment as controls (Figure 3A). Bak was predominantly expressed in mitochondrial fractions, which continued to increase until 8 h of observation during OGD treatment. No Bak expression was observed at any time point in cytoplasmic fractions. By contrast, Bax during OGD treatment remained unchanged in both cytoplasmic and mitochondrial fractions (Figure 3A). However, Bcl-xL increased significantly in mitochondrial fractions at 4 and 8 h under OGD as compared with OGD nontreated cells. Nevertheless, further OGD caused higher release of cytochrome-c into cytosolic fractions after 8 h OGD as compared with OGD non-treated cells, as well as 4 h OGD-treated cells (Figure 3A). Fluorescence immunostaining confirmed these data and showed loss of punctuate distribution of cytochrome-c in cells with 8 h OGD treatment (Figure 3B). Next, we treated the cells for 8 h OGD followed by mitochondrial and cytoplasmic fractionation of cellular proteins for western blotting (Figure 3C–G). Bax expression remained unchanged in cytoplasmic and mitochondrial fractions derived from ^{GFP}Sca-1^{+} cells and ^{Cx43}Sca-1^{+} cells (Figure 3C). By contrast, Bak in mitochondrial fractions was reduced in ^{Cx43}Sca-1^{+} cells as compared with ^{GFP}Sca-1^{+} cells, whereas Bak was insignificantly changed in the cytoplasmic fractions of each treatment group (Figure 3D). We observed moderately significant increases of Bcl-xL expression in mitochondrial fractions of ^{Cx43}Sca-1^{+} as compared with ^{GFP}Sca-1^{+} cells (Figure 3E). More importantly, however, the ratio between mitochondrial Bcl-xL and Bak was significantly higher in ^{Cx43}Sca-1^{+} cells (Figure 3F). These molecular events led to significantly lower level of cytosolic cytochrome-c in ^{Cx43}Sca-1^{+} cells ($p < 0.05$ vs ^{GFP}Sca-1^{+} cells).

Post-transplantation survival of ^{Cx43}Sca-1^{+} cells & preserved heart function

sry gene analysis by real-time PCR showed that ^{Cx43}Sca-1^{+} cells had higher survival post-transplantation in the infarcted myocardium ($p < 0.04$ vs ^{GFP}Sca-1^{+} cells; Figure 4A). DMEM-treated female animal hearts did not show *sry* gene expression and served as a negative control. TUNEL combined with desmin-specific immunostaining showed significantly lower numbers of TUNEL^{+} cardiomyocytes in ^{Cx43}Sca-1^{+} cell group 3 as compared with ^{GFP}Sca-1^{+} cell group 2 hearts (Figure 4B). Histological sections cut at the mid-papillary muscle level and stained with the Masson's trichrome method showed transmural infarction in all the animal groups (Figure 4C). However, infarction size at 4 weeks was significantly attenuated in ^{Cx43}Sca-1^{+} cell group 3 as compared with ^{GFP}Sca-1^{+} cell group 2 (33.7 ± 2.9% vs 39.8 ± 1.4%; $p < 0.05$) and DMEM group 1 (49.5 ± 2.8%; $p <$

0.05 vs group 3; Figure 4C). Moreover, higher number of cardiomyocytes and lower collagen contents were observed in the ^{Cx43}Sca-1^{+} cell group 3 as compared with the ^{GFP}Sca-1^{+} cell group 2 (Figure 4D). Histological evaluation of Masson's trichrome-stained tissue sections combined with TUNEL data revealed significantly higher numbers of cardiomyocytes in the center of the infarct in the ^{Cx43}Sca-1^{+} cell group 3 as compared with group 1 and group 2.

The animals were assessed for heart function by transthoracic echocardiography (Figure 4E–G). The indices of contractile function of the LV, including LVEF and LVFS, were higher in ^{Cx43}Sca-1^{+} cell group 3 as compared with ^{GFP}Sca-1^{+} cell group 2 (LVEF: 47.6 ± 2.5% vs 40.2 ± 0.9%, $p < 0.05$ and LVFS: 27.7 ± 1.2% vs 20.0 ± 1.6%, $p < 0.05$, respectively; Figure 4E & 4F). However, both the cell treatment groups had significantly preserved LV contractile function as compared with DMEM group 1 (LVEF: 28.3 ± 24.7%, $p < 0.05$ and LVFS: 13.5 ± 1.9%, $p < 0.05$). Transplantation of virus-infected cells also prevented remodeling of the LV as was apparent from more preserved LV end diastolic dimensions in comparison with group 1 and group 2. The smallest LV end-diastolic dimension was observed in ^{Cx43}Sca-1^{+} cell group 3 (5.6 ± 0.1 mm), which was significantly preserved, as compared with 6.5 ± 0.3 mm in ^{GFP}Sca-1^{+} cell group 2 ($p < 0.05$ vs group 3) and DMEM group 1 (8.1 ± 0.3 mm; $p < 0.05$ vs group 3; Figure 4G).

Discussion

Mitochondrial localization of Cx43 and its translocation under certain physiological and pathophysiological circumstances accounts for cytoprotection [4,11]. Failure of heterozygous Cx43-deficient mice (Cx43$^{+/-}$) to respond to ischemic as well as pharmacological preconditioning showed the importance of Cx43 in survival signaling [2,5,6]. However, using a similar Cx43$^{+/-}$ model, the putative role of Cx43 as a prerequisite for postconditioning was not validated, as loss of Cx43 did not alter infarct size reduction in postconditioned Cx43$^{+/-}$ mice as compared with wild-type animals [21]. The protective effects of Cx43 are independent of its role as a gap junction protein [7] and are mainly related to its mitochondria-specific localization [7,9]. Therefore, we constructed a high-efficiency Ad vector and standardized a protocol for optimal infectivity of stem cells to achieve mitochondria-specific *Cx43* transgene expression. Although both Ad-mito-GFP-FLAG and Ad-mito-Cx43-FLAG achieved 100% infection efficiency based on visual GFP expression, the amount of virus required for Ad-mito-GFP-FLAG and Ad-mito-Cx43-FLAG was different. Despite GFP being a convenient marker to show successful transgene delivery and expression efficiency, its reliability as a marker for quantitative estimation may lead to false estimation of the gene of interest. We therefore used a 3xFLAG tag fusion protein as a reporter for the detection and quantification of mitochondrial *Cx43* and *GFP* transgene expression subsequent to Ad-mito-Cx43-FLAG transduction. Our data clearly showed that when cells were infected with 100 μl of virus, the efficiency was excellent based upon GFP expression. Detection of FLAG accurately reflected whether GFP and Cx43 showed equimolar expression and helped to determine the optimal respective virus amounts to be used to achieve comparable expression, which made the subsequent study valid.

We selected three different amounts of virus for Ad-mito-GFP-FLAG and Ad-mito-Cx43-FLAG with comparable gene expression. We did not observe a dose-dependent toxicity in the range we tested. The cytoprotective effect of mito-Cx43-FLAG was obvious from cell morphology, TUNEL and caspase-3 activity assay. *In vivo* analysis showed improved survival of ^{Cx43}Sca-1^{+} post-transplantation, with concomitant attenuation of infarction size and improved global heart function.

The presence of mito-Cx43 and its antiapoptotic role have been attributed to signaling involving reactive oxygen species and the opening of mitochondria K^+-ATP channels [2,12,13]. There is evidence that mito-Cx43 in cardiomyocytes helps in mitochondrial potassium uptake [22]. However, due to a lack of the definitive molecular identity of K^+-ATP channels, how Cx43 affects mitochondrial function remains largely unknown. Our study on stem cells showed that mitochondria-specific targeting of Cx43 conferred similar cytoprotective effects by preventing cytochrome-c release from the mitochondria and caspase-3 activation [16]. These data were supported by published reports that mito-Cx43 was directly involved in the regulation of apoptosis during preconditioning, besides upregulation of the antiapoptotic Bcl-2 family of proteins [23]. On the same note, preconditioning with diazoxide protected neurons against ischemia via upregulation of Bcl-2 and simultaneous suppression of Bax translocation to the mitochondria, with resultant reductions in cytochrome-c release [24]. Computational analysis showed a BH3 motif in the Cx43 amino acid sequence at the C-terminal, an active region of interaction with numerous proteins including kinases, phosphatases, membrane receptors, cell signaling molecules and scaffolding proteins [25]. The BH3 motif is shared within the Bcl-2 family members and is crucial for their interaction with other molecules [26]. Bcl-2 members regulate apoptosis via regulating MOMPs, through which cytochrome-c is released into cytosol to activate the downstream caspase cascade [27,28]. Bax and Bak are the main players that homodimerize and/or heterodimerize to form MOMPs [20]. This process is prohibited by antiapoptotic Bcl-2 members and promoted by BH3-only Bcl-2 family members [29–31]. Whether mito-Cx43 is part of the Bcl-2 machinery that regulates cytochrome-c release is yet to be determined. Therefore, we investigated the dynamics of Bax, Bak and cytochrome-c changes under OGD and in response to mitochondrial preconditioning by targeted *Cx43* transgene expression. We observed higher cytochrome-c release from the mitochondria into cytosol in stem cells under OGD. Whereas Bax remained equally distributed between the mitochondria and cytosol, Bak showed a predominantly mitochondrial distribution. Bak upregulation in the mitochondria under OGD was accompanied by higher cytochrome-c release into cytosol. Mitochondrial preconditioning by targeted expression of Cx43 significantly reduced cytochrome-c release into cytosol, with a concomitant reduction in mitochondrial Bak and induction of Bcl-xL. These results are supported by a recent report that showed Bcl-xL retrotranslocates Bax from the mitochondria into cytosol [32]. MOMP formation was at least partially attributed to increased Bak in the mitochondria. These molecular events in preconditioned mitochondria involved an intricate interplay between antiapoptotic and proapoptotic Bcl-2 family members, or between the survival instincts of stem cells and apoptosis under OGD, which favored cell survival with mitochondrial *Cx43* transgene overexpression.

Despite these interesting data, there are some critical questions that remain unanswered. Firstly, the role of mito-Cx43 in preventing Bax/Bak heterodimerization under OGD and the possibility of whether mito-Cx43 physically interacted with Bcl-xL or other antiapoptotic Bcl-2 family members should be explored. An established in-depth causal relationship will provide mechanistic insight into our novel strategy of a subcellular preconditioning approach to stem cells based on mitochondrial targeting of Cx43. Second, it would be interesting to dissect whether mito-Cx43 was effective against both necrosis as well as apoptosis under OGD. It remains to be determined whether mito-Cx43 affects both outer as well as inner membrane pores, a possibility that is supported by recent findings [33]. However, based on our published data with the same mitochondrial localization sequence as used in our previously published study [16], we observed that transfected mito-Cx43 was expressed on the mitochondrial inner membrane. Moreover, functional alterations of Cx43 mutants, particularly those of the BH3 domain and α-helix, would be of great value in determining the critical amino acids that are functionally involved in cytoprotection.

Conclusion

Mitochondrial preconditioning by targeted *Cx43* transgene expression is a novel strategy to simulate the effects of preconditioning for improved donor stem cell survival in the infarcted heart. Transplantation of stem cells with preconditioned mitochondria would provide an alternative therapeutic option for acute myocardial infarction.

References

1. Duffy HS, Fort AG, Spray DC. Cardiac connexins: genes to nexus. Adv Cardiol. 2006; 42:1–17. [PubMed: 16646581]
2. Heinzel FR, Luo Y, Li X, et al. Impairment of diazoxide-induced formation of reactive oxygen species and loss of cardioprotection in connexin 43 deficient mice. Circ Res. 2005; 97(6):583–586. [PubMed: 16100048]
3. Ruiz-Meana M, Rodriguez-Sinovas A, Cabestrero A, Boengler K, Heusch G, Garcia-Dorado D. Mitochondrial connexin43 as a new player in the pathophysiology of myocardial ischaemia-reperfusion injury. Cardiovasc Res. 2008; 77(2):325–333. [PubMed: 18006437]
4. Boengler K, Dodoni G, Rodriguez-Sinovas A, et al. Connexin 43 in cardiomyocyte mitochondria and its increase by ischemic preconditioning. Cardiovasc Res. 2005; 67(2):234–244. [PubMed: 15919068]
5. Schwanke U, Konietzka I, Duschin A, Li X, Schulz R, Heusch G. No ischemic preconditioning in heterozygous connexin43-deficient mice. Am J Physiol Heart Circ Physiol. 2002; 283(4):H1740–H1742. [PubMed: 12234831]
6. Schwanke U, Li X, Schulz R, Heusch G. No ischemic preconditioning in heterozygous connexin 43-deficient mice – a further *in vivo* study. Basic Res Cardiol. 2003; 98(3):181–182. [PubMed: 12892084]
7. Padilla F, Garcia-Dorado D, Rodriguez-Sinovas A, Ruiz-Meana M, Inserte J, Soler-Soler J. Protection afforded by ischemic preconditioning is not mediated by effects on cell-to-cell electrical coupling during myocardial ischemia-reperfusion. Am J Physiol Heart Circ Physiol. 2003; 285(5):H1909–H1916. [PubMed: 12869372]
8. Garcia-Dorado D, Ruiz-Meana M, Padilla F, Rodriguez-Sinovas A, Mirabet M. Gap junction-mediated intercellular communication in ischemic preconditioning. Cardiovasc Res. 2002; 55(3): 456–465. [PubMed: 12160942]
9. Li X, Heinzel FR, Boengler K, Schulz R, Heusch G. Role of connexin 43 in ischemic preconditioning does not involve intercellular communication through gap junctions. J Mol Cell Cardiol. 2004; 36(1):161–163. [PubMed: 14734058]
10. Schulz R, Gres P, Skyschally A, et al. Ischemic preconditioning preserves connexin 43 phosphorylation during sustained ischemia in pig hearts *in vivo*. FASEB J. 2003; 17(10):1355–1357. [PubMed: 12759340]
11. Rodriguez-Sinovas A, Cabestrero A, Lopez D, et al. The modulatory effects of connexin 43 on cell death/survival beyond cell coupling. Prog Biophys Mol Biol. 2007; 94(1–2):219–232. [PubMed: 17462722]
12. Rodriguez-Sinovas A, Boengler K, Cabestrero A, et al. Translocation of connexin 43 to the inner mitochondrial membrane of cardiomyocytes through the heat shock protein 90-dependent TOM pathway and its importance for cardioprotection. Circ Res. 2006; 99(1):93–101. [PubMed: 16741159]
13. Rottlaender D, Boengler K, Wolny M, et al. Connexin 43 acts as a cytoprotective mediator of signal transduction by stimulating mitochondrial KATP channels in mouse cardiomyocytes. J Clin Invest. 2010; 120(5):1441–1453. [PubMed: 20364086]
14. Lu G, Haider HK, Jiang S, Ashraf M. Sca-1^{+} stem cell survival and engraftment in the infarcted heart: dual role for preconditioning-induced connexin-43. Circulation. 2009; 119(9):2587–2596. [PubMed: 19414636]

15. Lu G, Ashraf M, Haider KH. Insulin-like growth factor-1 preconditioning accentuates intrinsic survival mechanism in stem cells to resist ischemic injury by orchestrating protein kinase cα-erk1/2 activation. Antioxid Redox Signal. 2012; 16(3):217–227. [PubMed: 21923556]
16. Lu G, Haider H, Porollo A, Ashraf M. Mitochondria-specific transgenic overexpression of connexin-43 simulates preconditioning-induced cytoprotection of stem cells. Cardiovasc Res. 2010; 88(2):277–286. [PubMed: 20833648]
17. Apostolova N, Blas-Garcia A, Esplugues JV. Mitochondria sentencing about cellular life and death: a matter of oxidative stress. Curr Pharm Des. 2011; 17(36):4047–4060. [PubMed: 22188454]
18. Heusch G, Boengler K, Schulz R. Cardioprotection: nitric oxide, protein kinases, and mitochondria. Circulation. 2008; 118(19):1915–1919. [PubMed: 18981312]
19. Luo J, Deng ZL, Luo X, et al. A protocol for rapid generation of recombinant adenoviruses using the AdEasy system. Nat Protoc. 2007; 2(5):1236–1247. [PubMed: 17546019]
20. Jurgensmeier JM, Xie Z, Deveraux Q, Ellerby L, Bredesen D, Reed JC. Bax directly induces release of cytochrome c from isolated mitochondria. Proc Natl Acad Sci USA. 1998; 95(9):4997–5002. [PubMed: 9560217]
21. Heusch G, Buchert A, Feldhaus S, Schulz R. No loss of cardioprotection by postconditioning in connexin 43-deficient mice. Basic Res Cardiol. 2006; 101(4):354–356. [PubMed: 16568250]
22. Miro-Casas E, Ruiz-Meana M, Agullo E, et al. Connexin43 in cardiomyocyte mitochondria contributes to mitochondrial potassium uptake. Cardiovasc Res. 2009; 83(4):747–756. [PubMed: 19460776]
23. Meller R, Minami M, Cameron JA, et al. CREB-mediated Bcl-2 protein expression after ischemic preconditioning. J Cereb Blood Flow Metab. 2005; 25(2):234–246. [PubMed: 15647742]
24. Liu D, Lu C, Wan R, Auyeung WW, Mattson MP. Activation of mitochondrial ATP-dependent potassium channels protects neurons against ischemia-induced death by a mechanism involving suppression of Bax translocation and cytochrome c release. J Cereb Blood Flow Metab. 2002; 22(4):431–443. [PubMed: 11919514]
25. Singh D, Lampe PD. Identification of connexin-43 interacting proteins. Cell Commun Adhes. 2003; 10(4–6):215–220. [PubMed: 14681019]
26. Kelekar A, Thompson CB. Bcl-2-family proteins: the role of the BH3 domain in apoptosis. Trends Cell Biol. 1998; 8(8):324–330. [PubMed: 9704409]
27. Kluck RM, Bossy-Wetzel E, Green DR, Newmeyer DD. The release of cytochrome c from mitochondria: a primary site for Bcl-2 regulation of apoptosis. Science. 1997; 275(5303):1132–1136. [PubMed: 9027315]
28. Yang J, Liu X, Bhalla K, et al. Prevention of apoptosis by Bcl-2: release of cytochrome c from mitochondria blocked. Science. 1997; 275(5303):1129–1132. [PubMed: 9027314]
29. Willis SN, Fletcher JI, Kaufmann T, et al. Apoptosis initiated when BH3 ligands engage multiple Bcl-2 homologs, not Bax or Bak. Science. 2007; 315(5813):856–859. [PubMed: 17289999]
30. Puthalakath H, Strasser A. Keeping killers on a tight leash: transcriptional and post-translational control of the pro-apoptotic activity of BH3-only proteins. Cell Death Differ. 2002; 9(5):505–512. [PubMed: 11973609]
31. Cheng EH, Wei MC, Weiler S, et al. BCL-2, Bcl-xL sequester BH3 domain-only molecules preventing Bax- and Bak-mediated mitochondrial apoptosis. Mol Cell. 2001; 8(3):705–711. [PubMed: 11583631]
32. Edlich F, Banerjee S, Suzuki M, et al. Bcl-xL retrotranslocates Bax from the mitochondria into the cytosol. Cell. 2011; 145(1):104–116. [PubMed: 21458670]
33. Azarashvili T, Baburina Y, Grachev D, et al. Calcium-induced permeability transition in rat brain mitochondria is promoted by carbenoxolone through targeting connexin43. Am J Physiol Cell Physiol. 2011; 300(3):C707–C720. [PubMed: 21148408]

Executive summary

- Mitochondrial translocation of connexin-43 (Cx43) constitutes an integral part of growth factor preconditioning of stem cells.
- The cytoprotective effects of growth factor preconditioning can be simulated by mitochodria-specific targeting of the *Cx43* transgene.
- Our data provide the first evidence of subcellular preconditioning via mitochondria-specific targeting of Cx43.
- We report successful construction of an adenoviral vector encoding for Cx43 with a mitochondria-specific localization signal.
- Stem cells with mitochondria-specific localization of Cx43 showed significantly improved survival upon subsequent exposure to lethal anoxia.
- Mitochondria-specific Cx43 overexpression reduced cytochrome-c release and shifted the balance between mitochondrial Bak and Bcl-xL.
- Stem cells with mitochondria-specific Cx43 overexpression showed improved survival post-transplantation in the ischemic heart.

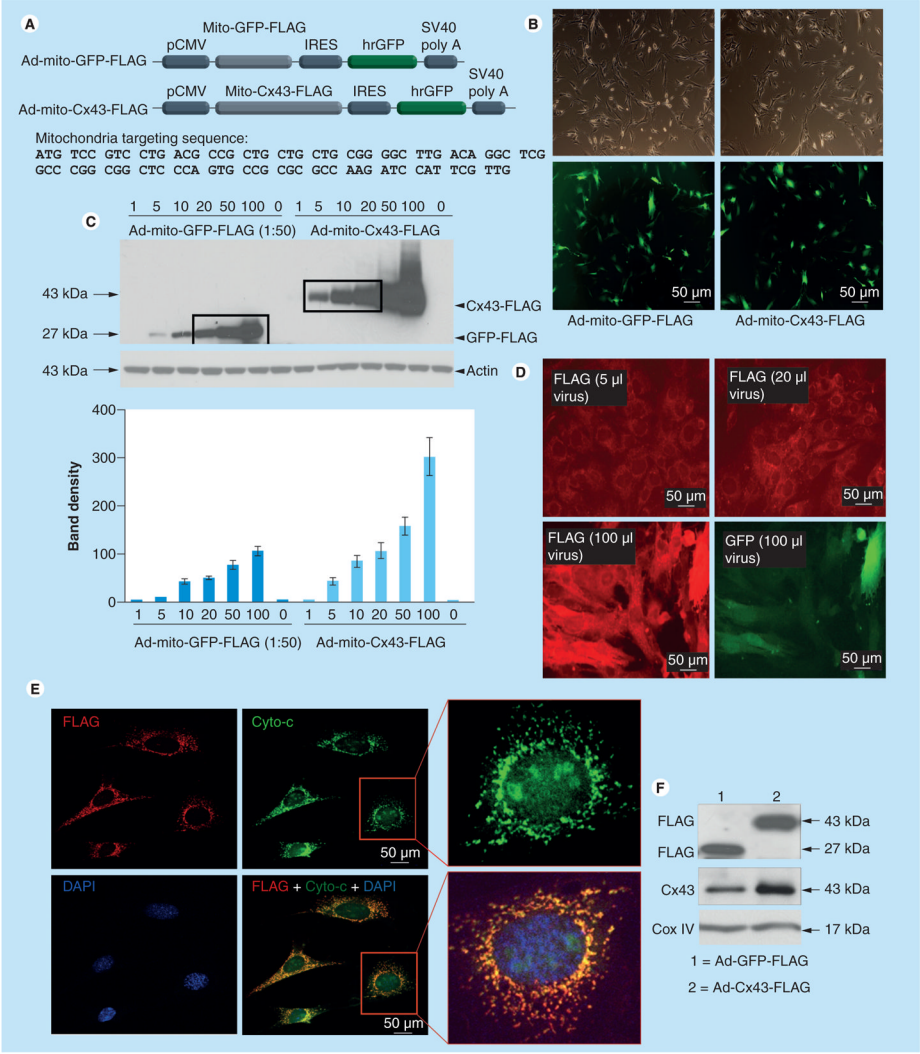

Figure 1. Construction and characterization of adenoviral vectors

(A) Diagram of recombinant Ad vectors for mito-GFP-FLAG (control) and mito-Cx43-FLAG. Mitochondrial targeting sequences were fused in-frame upstream of GFP and Cx43 and three repeats of FLAG were fused in-frame downstream of GFP and Cx43 in their respective vector constructs. There was a second open reading frame encoding humanized recombinant GFP. These Ad vectors were later used for genetic modulation of Sca-1$^+$ cells. **(B)** Phase-contrast and fluorescence photomicrographs showing successfully transduced Sca-1$^+$ cells with respective Ad vectors. Transduction efficiency was almost 100%. **(C)** Sca-1$^+$ cells were infected with increasing amounts of Ad-mito-GFP-FLAG and Ad-mito-Cx43-FLAG for titration of Ad vector concentration for optimal transduction efficiency with little cellular damage. Cell lysate samples were analyzed by western blots to detect FLAG. Densitometry showed increasing levels of mito-FLAG in ^{Cx43}Sca-1$^+$ cells as compared with ^{GFP}Sca-1$^+$ cells using nontransduced Sca-1$^+$ cells as baseline controls for FLAG expression. Sca-1$^+$ cells infected with 5, 10 and 20 µl of Ad-mito-Cx43-FLAG expressed similar amounts of FLAG as Sca-1$^+$ cells infected with 20, 50 and 100 µl of Ad-mito-GFP-FLAG, respectively. **(D)** Sca-1$^+$ cells infected with various amounts of Ad-mito-Cx43-FLAG and immunostained with anti-FLAG primary antibody and detected with Alexa Fluor® 546-conjugated secondary antibody (Invitrogen, CA, USA). Pictures for FLAG

immunostaining were all taken with 0.2 s exposure for comparison. Pictures for GFP were only taken for cells infected with 100 μl of virus since cells transduced with lower viral vector amounts did not show visible green fluorescence. **(E)** Confocal images of Sca-1^+ immunostained for anti-FLAG (red) and anti-Cyto-c (green). DAPI was used to visualize nuclei. The merged image shows punctuate distribution of FLAG (red) colocalized with Cyto-c (green). **(F)** Western blotting of mitochondrial subfractions of ^{Cx43}Sca-1^+ cells, and ^{GFP}Sca-1^+ cells respectively. The membrane was probed with anti-FLAG and anti-Cx43 antibodies. Significantly higher levels of Cx43 were observed in the mitochondrial fraction of ^{Cx43}Sca-1^+ cells. Cox IV was used as a mitochondrial fraction marker.
Ad: Adenoviral; Cx43: Connexin-43; Cyto-c: Cytochrome-c; IRES: Internal ribosomal entry site; Mito: Mitochondrial.

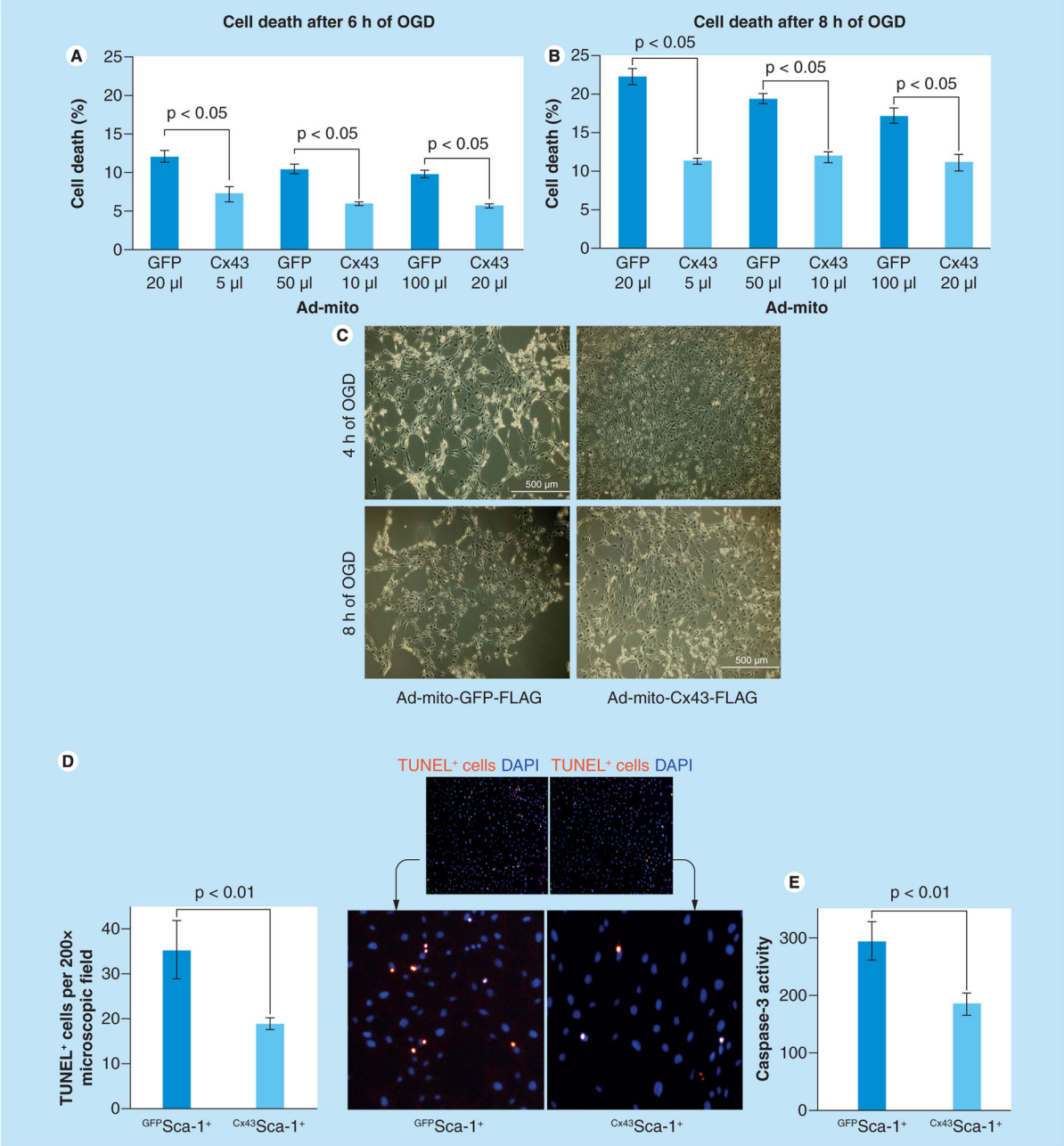

Figure 2. Prosurvival effects of mitochondrial connexin-43 on Sca-1$^+$ cells under oxygen–glucose deprivation

(A) Lactate dehydrogenase assay using conditioned medium obtained from ^{Cx43}Sca-1$^+$ cells and ^{GFP}Sca-1$^+$ cells subjected to either 6 or 8 h anoxia. The amount of Ad-mito-GFP-FLAG and Ad-mito-Cx43-FLAG used for transduction was determined from the titration experiment from Figure 1B to achieve relatively equal expression of FLAG. Cell death was less in ^{Cx43}Sca-1$^+$ cells from all three different Ad vector doses used for transduction ($p < 0.05$ for all comparisons vs ^{GFP}Sca-1$^+$ at both time points). **(C)** Phase-contrast microscopy showing maintenance of cellular morphology in ^{Cx43}Sca-1$^+$ cells as compared with ^{GFP}Sca-1$^+$ cells. **(D)** Fluorescence photomicrographs of ^{GFP}Sca-1$^+$ and ^{Cx43}Sca-1$^+$ cells after TUNEL (red). The nuclei were stained with DAPI (blue). The number of

TUNEL^{+} ^{GFP}Sca-1^{+} cells was significantly higher as compared with ^{Cx43}Sca-1^{+} cells under 8 h anoxia (original magnification ×200). **(E)** ^{Cx43}Sca-1^{+} cells showed low caspase-3 activity as compared with ^{GFP}Sca-1^{+} cells ($p < 0.05$) under 8 h anoxia.
Ad: Adenoviral; Cx43: Connexin-43; Mito: Mitochondrial; OGD: Oxygen–glucose deprivation; TUNEL: Terminal deoxynucleotidyl transferase dUTP nick end labeling.

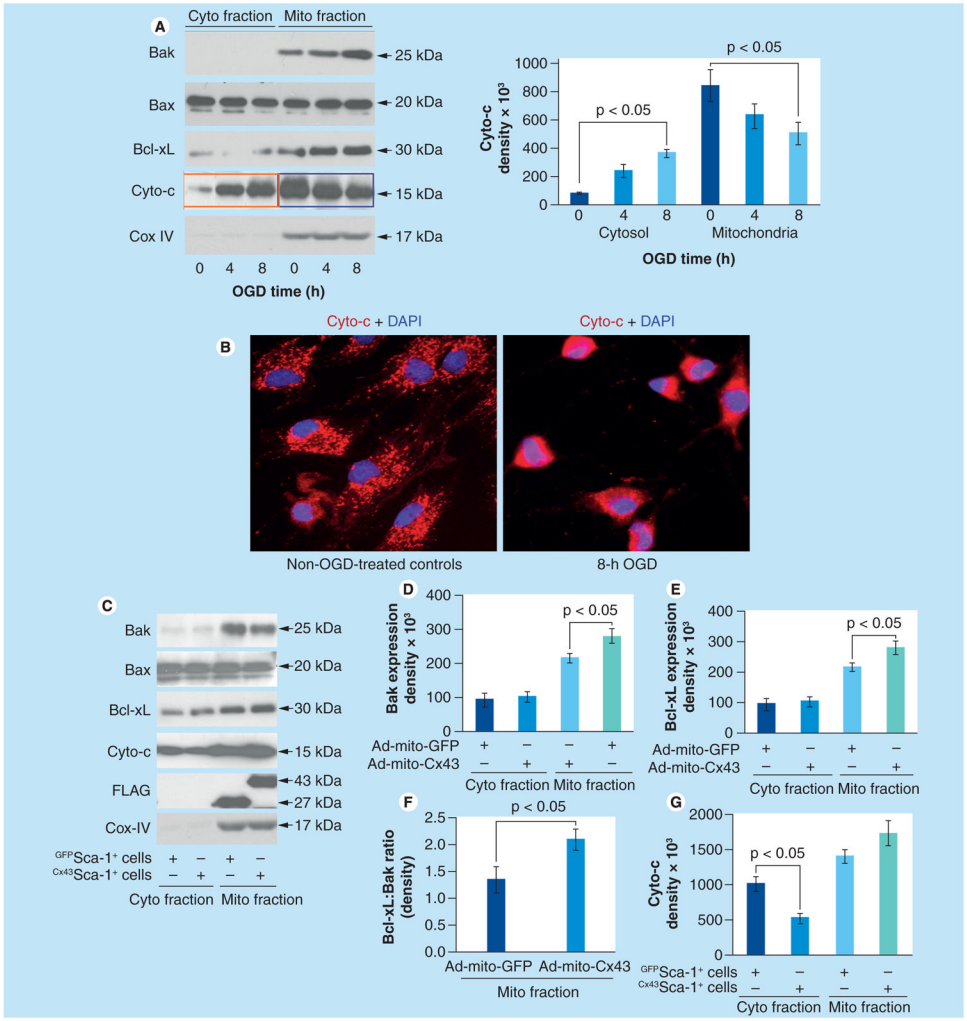

Figure 3. Mitochondrial connexin-43 alters dynamics of antiapoptotic Bcl-2 family members

(A) Western blotting using cytoplasmic and mitochondrial protein fractions from ^{Cx43}Sca-1^{+} cells after OGD treatment for 0, 4 and 8 h. Increasingly higher expression of Bak, Cyto-c and Bcl-xL was observed in mitochondrial fractions at 4 and 8 h of OGD treatment as compared with cytoplasmic fractions. Cox IV was used as a loading control and to show the purity of cytoplasmic and mitochondrial fractions. **(B)** Fluorescence immunostaining of Sca-1^{+} cells exposed to 8 h OGD showed loss of punctuate distribution of Cyto-c. The nuclei were visualized with DAPI staining (blue; original magnification ×40). **(C–G)** Western blots of cytoplasmic and mitochondrial protein fractions from ^{Cx43}Sca-1^{+} cells and ^{GFP}Sca-1^{+} cells after 8 h OGD treatment showed that Bax expression in both mitochondrial and cytoplasmic fractions remained unchanged. However, Bcl-xL expression increased significantly in mitochondrial fractions of ^{Cx43}Sca-1^{+} as compared with ^{GFP}Sca-1^{+} cells, whereas expression of both Bak and Bcl-xL in cytoplasmic fractions of ^{Cx43}Sca-1^{+} cells remained unchanged. The Bcl-xL:Bak ratio was significantly higher in mitochondrial fractions of ^{Cx43}Sca-1^{+} cells. These molecular events significantly favored reduced Cyto-c release into cytosolic fractions of ^{Cx43}Sca-1^{+} cells. Cox IV was used as a loading control and to show the purity of cytoplasmic and mitochondrial fractions. The graphs show band intensity from three independent experiments.

Ad: Adenoviral; Cx43: Connexin-43; Cyto: Cytoplasmic; Cyto-c: Cytochrome-c; Mito: Mitochondrial; OGD: Oxygen–glucose deprivation.

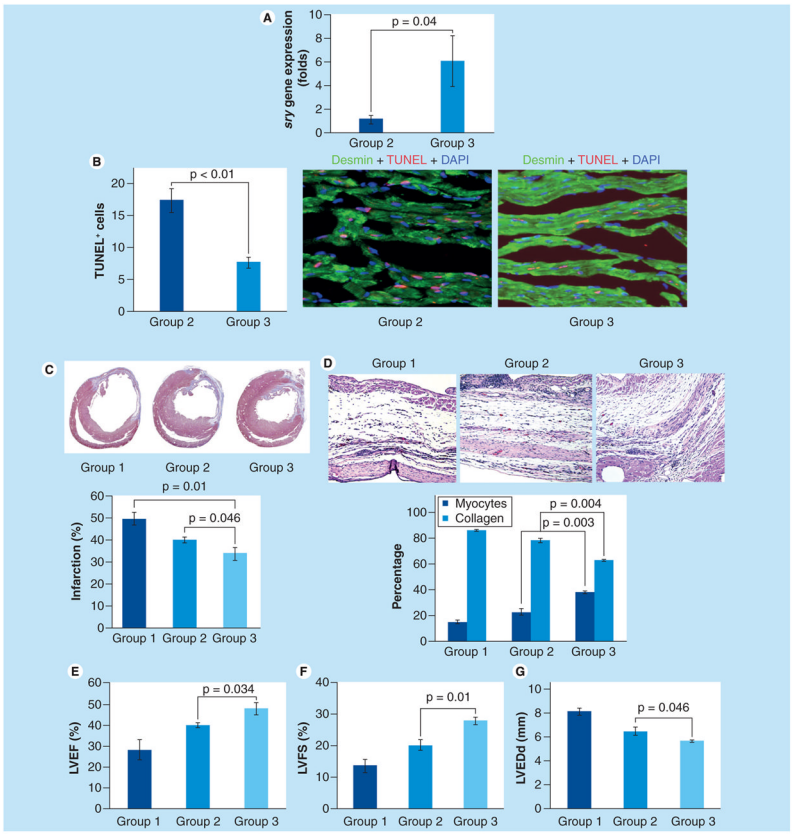

Figure 4. Connexin-43 Sca-1$^+$ cells had significantly higher survival in infarcted animal hearts

(A) Rats sacrificed on day 7 after their respective treatment were used for *sry* gene expression in the left ventricular tissue samples. Real-time PCR for the *sry* gene showed higher survival of ^{Cx43}Sca-1$^+$ cells as compared with ^{GFP}Sca-1$^+$ group 2 ($p < 0.04$). DMEM group 1 animal hearts did not show *sry* gene expression and served as negative controls. **(B)** Representative images from the peri-infarct region of histological tissue section after TUNEL. TUNEL was performed on histological sections of the hearts collected on day 3 from ^{GFP}Sca-1$^+$ group 2 and ^{Cx43}Sca-1$^+$ group 3 animals. Cardiomyocytes were stained with desmin-specific antibody (green). The nuclei were visualized by DAPI staining (blue). The number of TUNEL$^+$ (red) cardiomyocytes was significantly lower in group 3 animal hearts as compared with group 2. **(C)** Masson's trichrome staining of histological sections showed that infarction size was reduced in ^{Cx43}Sca-1$^+$ group 3 as compared with ^{GFP}Sca-1$^+$ group 2 and DMEM group 1 ($p < 0.05$). **(D)** The number of myocytes in the center of the infarct was higher and collagen contents were lower in ^{Cx43}Sca-1$^+$ group 3 animal hearts ($p < 0.05$ vs groups 1 and group 2). **(E–G)** ^{Cx43}Sca-1$^+$ cells showed significantly improved **(E)** LVEF, **(F)** LVFS and **(G)** reduced LVEDd as compared with ^{GFP}Sca-1$^+$ group 2 and DMEM group 1.

Cx43: Connexin-43; LVEDd: Left ventricular end diastolic dimension; LVEF: Left ventricular ejection fraction; LVFS: Left ventricular fractional shortening; TUNEL: Terminal deoxynucleotidyl transferase dUTP nick end labeling.